American Genetic Association

OXFORD

Symposium Article

Heat challenge elicits stronger physiological and gene expression responses than starvation in symbiotic *Oculina arbuscula*

Hanny E. Rivera[iD], Carlos A. Tramonte[iD], Jason Samaroo[iD], Hayden Dickerson[iD], Sarah W. Davies*,[iD]

[1]Department of Biology, Boston University, Boston, MA 02215, USA
*Corresponding author. Email: daviessw@bu.edu

Corresponding Editor: Kelly Zamudio

Abstract

Heterotrophy has been shown to mitigate coral–algal dysbiosis (coral bleaching) under heat challenge, but the molecular mechanisms underlying this phenomenon remain largely unexplored. Here, we quantified coral physiology and gene expression of fragments from 13 genotypes of symbiotic *Oculina arbuscula* after a 28-d feeding experiment under (1) fed, ambient (24 °C); (2) unfed, ambient; (3) fed, heated (ramp to 33 °C); and (4) unfed, heated treatments. We monitored algal photosynthetic efficiency throughout the experiment, and after 28 d, profiled coral and algal carbohydrate and protein reserves, coral gene expression, algal cell densities, and chlorophyll-a and chlorophyll-c_2 pigments. Contrary to previous findings, heterotrophy did little to mitigate the impacts of temperature, and we observed few significant differences in physiology between fed and unfed corals under heat challenge. Our results suggest the duration and intensity of starvation and thermal challenge play meaningful roles in coral energetics and stress response; future work exploring these thresholds and how they may impact coral responses under changing climate is urgently needed. Gene expression patterns under heat challenge in fed and unfed corals showed gene ontology enrichment patterns consistent with classic signatures of the environmental stress response. While gene expression differences between fed and unfed corals under heat challenge were subtle: Unfed, heated corals uniquely upregulated genes associated with cell cycle functions, an indication that starvation may induce the previously described, milder "type B" coral stress response. Future studies interested in disentangling the influence of heterotrophy on coral bleaching would benefit from leveraging the facultative species studied here, but using the coral in its symbiotic and aposymbiotic states.

Key words: climate change, coral symbiosis, environmental stress response, facultative coral, gene expression, heterotrophy

Introduction

The majority of tropical reef-building corals form obligate symbiotic relationships with endosymbiotic algae in the family Symbiodiniaceae, and this relationship forms the foundation for the ecological success coral reefs have experienced over millions of years (Muscatine and Porter 1977; Glynn 1996; Hughes et al. 2017). In this relationship, the coral host relies on photosynthetically fixed carbon (photosynthates) and amino acids from the algae in order to thrive in nutrient-poor tropical waters (Muscatine and Porter 1977). In fact, these algae can provide upwards of 90% of their coral host's energetic demands (Muscatine et al. 1981). In exchange, the algae receive a protected and light-exposed endosymbiotic residence, inorganic nutrients, and host CO_2 concentration mechanisms that increase photosynthetic efficiency (Muscatine and Cernichiari 1969; Muscatine 1990; Barott et al. 2015).

Unfortunately, this symbiosis can be disrupted by a variety of stressors, though it is largely accepted that rising ocean temperatures pose the single greatest threat to the future of coral reefs through the induction of bleaching (Hughes et al. 2017, 2018). The loss of symbionts deprives the coral host of its symbiont-derived sugars and many corals cannot survive when bleached for extended periods of time. Mass bleaching events have led to the rapid degradation of coral reefs globally over the past decades and are expected to continue increasing in frequency and severity as climate change progresses (Normile 2016; Pernice and Hughes 2019).

If a bleached coral is to survive, it must rely on alternative carbon sources to meet its energy needs, which include tapping into stored energy reserves (proteins, lipids, carbohydrates) and heterotrophy (reviewed in Houlbrèque and Ferrier-Pagès 2009). Heterotrophy has been shown to mitigate the negative effects of thermal stress in both tropical (Grottoli et al. 2006; Hughes and Grottoli 2013; Tremblay et al. 2016; Morris et al. 2019; Conti-Jerpe et al. 2020) and subtropical coral species (Aichelman et al. 2016). In addition to bleaching resistance, overall enhanced coral health has also been linked to heterotrophy with fed corals having higher growth rates (Miller 1995; Reynaud-Vaganay et al. 2002; Rodolfo-Metalpa et al. 2008;

Aichelman et al. 2016; Levy et al. 2016; Conlan et al. 2017), being better able to recover from wounding (Burmester et al. 2018), and having higher survivorship in general (Anthony et al. 2009; Toh et al. 2014; Conlan et al. 2017) relative to unfed corals. Importantly, recent work using stable isotope analyses to identify coral trophic niches suggests that corals that are more reliant on heterotrophy are more bleaching resistant and, therefore, more likely to outperform more autotrophic corals under climate change (Conti-Jerpe et al. 2020), highlighting an urgent need to better understand the role of heterotrophy and bleaching.

The physiological and molecular responses of tropical reef-building corals under thermal challenges have been widely explored (reviewed in Cziesielski et al. 2019). Short-term thermal challenges in coral consistently cause the upregulation of heat-shock proteins, apoptotic response pathways, superoxide dismutase, ubiquitin pathways, and genes associated with ion transport and metabolism (Meyer et al. 2011; Barshis et al. 2013; Dixon et al. 2015; Hawkins et al. 2015; Avila-Magaña et al. 2021), with these responses shifting to broad-scale downregulation of basic metabolic processes under long-term challenges (Vidal-Dupiol et al. 2014; Davies et al. 2016). Many of these studies have focused on tropical reef-building corals in the genus *Acropora*. A recent meta-analysis of various stress challenges including thermal stress found there were two distinct environmental stress responses—one that was observed under high-intensity stress (type A) and another more subtle response characteristic of lower-intensity stress (type B) (Dixon et al. 2020). While these stress responses have been less explored in subtropical and temperate coral species, Wuitchik et al. (2021) profiled gene expression under divergent thermal challenges and found the same molecular signatures of stress were consistently uncovered in an aposymbiotic, temperate reef-building coral (*Astrangia poculata*). These studies have been central to building our understanding of environmental stress responses in corals and the mechanisms underlying the maintenance and loss of symbiosis.

While the molecular signature of heat challenge has been widely explored in corals, the gene expression signatures of heterotrophy and how they may mediate other stress responses remain largely unexplored (see Bay et al. 2013; Levy et al. 2016). Here, we examined the physiological and gene expression responses of the subtropical facultative coral, *Oculina arbuscula*, under heat challenge and heterotrophy to understand how heterotrophy influences the coral host and the algal symbiont response to heat challenge. Fragments from 14 colonies were placed under four treatment conditions: (1) fed, ambient (24 °C, control); (2) unfed, ambient; (3) fed, heated (ramp to 33 °C); and (4) unfed, heated for 28 d. At the end of the experiment, a panel of host and symbiont phenotypes were characterized and genome-wide gene expression profiling via TagSeq was performed to identify the molecular mechanisms underlying these responses.

Materials and methods

Colony collection

Colonies (*N* = 14) of *O. arbuscula* were collected off the coast of North Carolina at the Radio Island Jetty (34° 42.520′ N, 76° 40.796′ W) in 2018 (NC Division of Marine Fisheries Permit #1627488). Colonies were fragmented using a tabletop diamond saw to create genotypic replicates, which were affixed to ceramic bases using underwater glue and maintained under common garden conditions for ~1.5 yr in the Davies Marine Population Genomics Lab at Boston University.
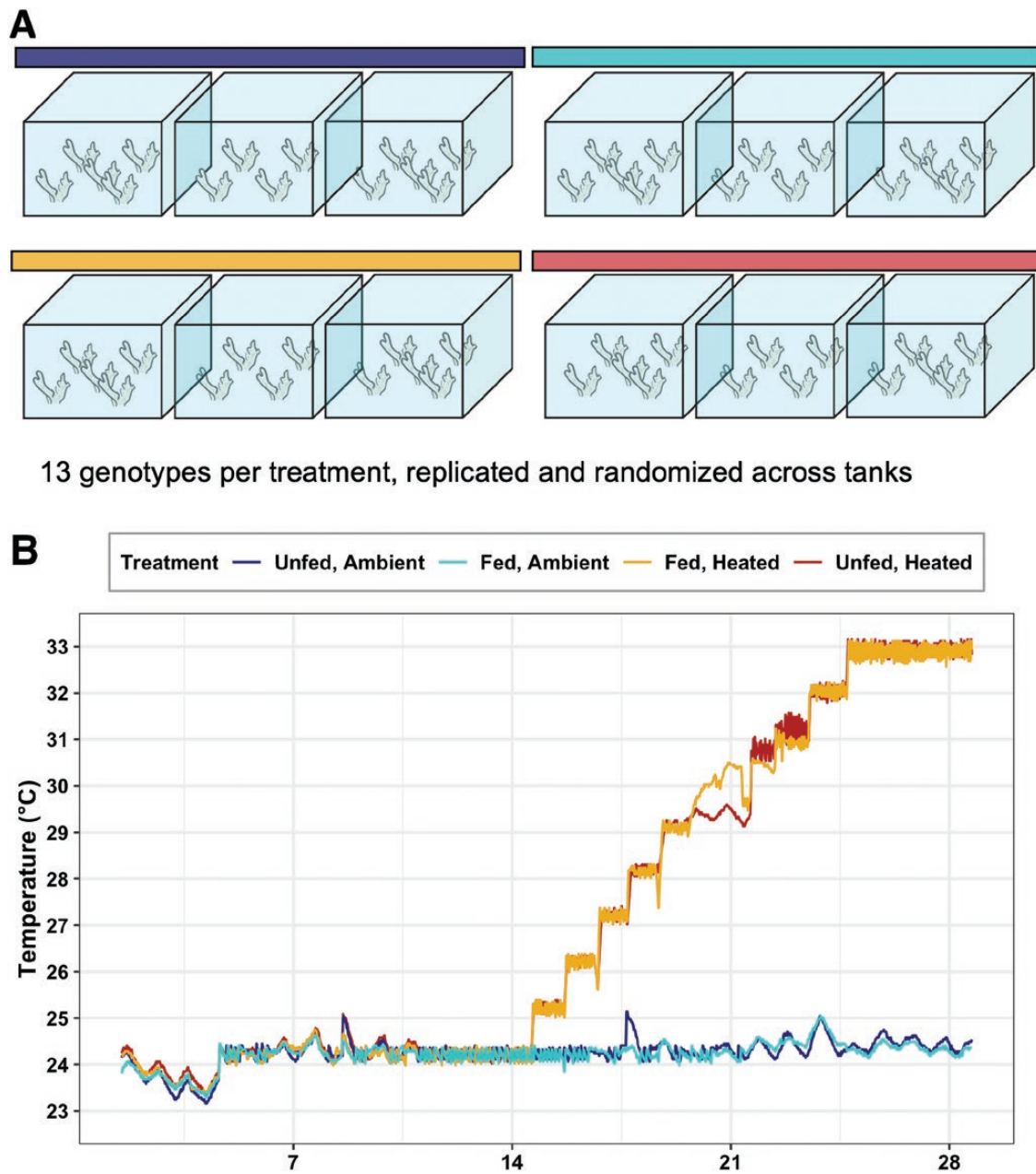
Experimental setup

Four fragments of each of the 13 genotypes (two of the colonies were found to be clones during a different study; see Rivera and Davies 2021) were assigned to one of four temperature/feeding treatments: (1) fed, ambient (control); (2) unfed, ambient; (3) fed, heated; and (4) unfed, heated (total *N* = 52 fragments). Each treatment had three tanks, each of which housed four to five coral fragments. Fragments of each genotype were randomly assigned to tanks within a treatment using a random number generator (Fig. 1A). Fragments were rotated through fixed positions in the tank weekly to minimize microenvironmental differences within tanks. Each tank was illuminated with a Hydra-32HD, Aquaillumination™ LED light on a 12:12 light–dark cycle, which included a 1-h ramp up and ramp down of light intensity to simulate sunrise/sunset. Lights were configured to have identical spectral qualities and ~45 umol photons m^{-2} s^{-1}. Each tank had a water circulation pump and 50% water changes were conducted weekly. Apex™ control systems were used to regulate temperatures in 20-gallon aquarium tanks filled with artificial Instant Ocean™ seawater at ~ 33 PSU salinity. HOBO™ tidbit loggers were maintained in each treatment sump and temperatures were logged every 15 min. Temperature and salinity were also checked manually at least every other day using a YSI Pro 30 meter. Salinity in all treatments ranged between 31 and 35 PSU throughout the course of the experiment.

Fed fragments were offered 1 ml of Reef-Roids™ powder dissolved in 8 ml of seawater daily, using a small squirt bottle to direct food over coral fragments. Each coral was fed ~0.25 ml of food per day in the evening to better simulate crepuscular feeding activity. After beginning feeding treatments, all corals were maintained at ambient temperature levels (24 °C) for 1.5 wk, prior to beginning temperature ramps for the two heated treatments. In heated treatments, temperatures were increased stepwise by approximately 1 °C per day for 10 d, until reaching a maximum temperature of 33 °C. Treatments were then maintained at 33 °C for 4 d, at which time the experiment ended (Fig. 1B).

Holobiont physiology

Symbiont photosynthetic efficiency (F_v/F_m) was measured using a Walz Junior-PAM™ four times throughout the experiment (weekly on days 7, 14, 21, and 28). Corals were dark-acclimated for at least 20 min prior to measurements and all measurements were conducted in the dark. Three replicate F_v/F_m measurements were taken for each fragment and averaged within each time point.

At the end of the experiment, each fragment was photographed to document live and dead tissue areas and then flash frozen in liquid nitrogen and immediately stored at –80 °C. Two fragments died prior to the end of the experiment, leaving 50 fragments remaining. At the beginning of processing, a small tissue sample (<2 cm^2) from each fragment was removed for RNA extraction (see below). Fragments were then thawed and the tissue was removed via airbrushing using an airgun with sterile saltwater. Tissue slurry was homogenized for 3 min using a handheld tissue homogenizer (Tissue-Tearor Model 985370, BioSpec Products, Inc.).

Fig. 1. (A) Experimental design showing tank setup and coral distributions across tanks and experimental treatments. Each treatment had three replicate tanks, with a common temperature controller and sump. Lighting regimes were identical across tanks. (B) Temperatures of experimental treatments throughout the 28-d experiment. P indicates when F_v/F_m measurements were taken and the asterisk indicates when corals were flash frozen for phenotypic and gene expression analyses.

An aliquot of the slurry was then separated for symbiont density assessments (see below) and the remaining slurry was centrifuged at 4,400 rpm for 3 min to pellet symbiont cells. The supernatant was decanted and represents the coral "host" fraction for physiology measurements. The symbiont pellet was resuspended in 5 ml of sterile seawater. Both host and symbiont slurries were bead blasted using Sigma glass beads and a Fisher Scientific Bead Mill 24 at 6 m/s for 2 min.

Airbrushed coral skeletal fragments were 3D scanned to assess surface area using an EIN-SCAN SE tabletop 3D scanner with the HDR and texture scanning options enabled. Each fragment was scanned two to three times to produce a complete watertight mesh of the coral surface. Scans were then imported into MeshLab™ software. Final photographs were consulted to carefully select areas of the skeleton containing live tissue using the z-paintbrush tool in MeshLab. Once all live tissue areas were selected, the total live surface area was calculated by the software.

Symbiont densities (cells/cm^2) were measured for three replicate 10 μl tissue slurry aliquots per fragment using a hemocytometer under a light microscope. Counts were averaged, extrapolated to the total slurry volume, and normalized to live coral tissue surface area.

Host and symbiont protein concentrations (mg/cm^2) were assessed using Bradford assays with a Bovine Albumin Serum (BSA) standard for reference. 6.4 μl of the sample was added

to 73.6 µl of artificial seawater along with 80 µl of Bradford reagent. Samples were mixed and a Synergy H1™ Microplate Reader spectrophotometer was used to measure absorbance at 595 nm. Coral protein concentrations were calculated using the standard curve from BSA and normalized to the living coral surface area.

Host and symbiont carbohydrate concentrations (mg/cm²) were assessed using the phenol–sulfuric acid method (Masuko et al. 2005), with a D-glucose standard for reference. For each sample, 10 µl was mixed with 40 µl of sterile seawater, 150 µl of sulfuric acid, and 30 µl of 5% phenol. Samples were incubated at 90 °C for 5 min using a water bath and then at room temperature for 5 min in the dark. Absorbance at 490 nm was measured using a Synergy H1™ Microplate Reader spectrophotometer. Carbohydrate concentrations were then calculated using a D-glucose standard curve and normalized to the living coral surface area.

To quantify symbiont chlorophyll-a and chlorophyll-c_2 pigments (µg/cm²), symbiont tissue extracts were pelleted and incubated in 1 ml of 90% acetone overnight in the dark at 4 °C. For each sample, three 200 µl aliquots were assayed using a Synergy H1™ Microplate Reader spectrophotometer to measure absorbance at 630 and 663 nm. Absorbance values were converted to pigment concentrations using the formulas from Jeffrey and Haxo (1968), chlorophyll-a = 13.31(Absorbance$_{663}$) − 0.27(Absorbance$_{630}$); chlorophyll-c_2 = −8.37(Absorbance$_{663}$) + 51.72(Absorbance$_{630}$), with an additional factor applied to account for the lower volume used in our assay (200 µl) in relation to the original (1 ml) and normalized to the living coral surface area.

Statistical analyses

Physiology data were analyzed in R using generalized linear models through the formulation *lmer*(response_variable~treatment + [1|genotype]) for each physiological response variable, where coral genotype is treated as a random effect. For PAM data, the individual coral fragment was used as the random effect to account for repeated measures across the experiment. For each model output where treatment showed a significant ($p < 0.05$) effect, the differences between each pairwise set of treatments were compared using the general linear hypothesis *glht*() function in the r package *multcomp*, which uses post hoc Tukey tests to contrast pairs while correcting for multiple comparisons (Hothorn et al. 2008). Overall differences among treatments for all end-of-experiment (day 28) host and symbiont physiology data were also explored using a principal component analysis (PCA). The effect of treatment was tested using a PERMANOVA with the *adonis()* function in the R package *vegan* using Euclidean distances. All scripts used for analyses are available in Supplementary Materials and on the first author's github repository (see Data Accessibility statement).

RNA extraction and gene expression analyses

Coral tissue samples from the end of the experiment were processed using the RNAqueous RNA extraction kit (Ambion) following the manufacturer's recommendations, with a modified bead beating step added to the lysis stage. Samples were homogenized twice using a bead beater at 5 m/s for 30 s. Extracted RNA quantity was assessed using a DeNovix DS-11+ spectrophotometer and RNA quality was assessed on a 1% agarose gel to visualize ribosomal RNA bands. Any

excess DNA was removed through DNase 1 (Ambion) at digestion at 37 °C for 30 min. Only 23 samples had sufficient RNA quantity and quality to meet library preparation requirements. RNA libraries were created using approximately 1.5 µg of RNA per sample. RNA was first heat degraded for 10 min at 75 °C. First-strand cDNA synthesis was accomplished using a template-switching oligo and SMARTScribe reverse transcriptase (Clontech) incubated at 42 °C for 1 h and 65 °C for 15 min. cDNA was then PCR-amplified, using Tagseq primers (3ILL-30TV; 5ILL) and Titanium Taq (Meyer et al. 2011). AmPure beads cleaned PCR products and libraries were normalized to have equal cDNA concentration. Samples were barcoded, pooled, and then size selected (400 to 500 base pair fragments) using an agarose gel extraction. Samples were sequenced at the Tufts University Core Facility on an Illumina Hiseq 2500, as single-end 50 base pair reads.

Demultiplexed reads were mapped to a concatenated *O. arbuscula* and *Breviolum psygmophillum* transcriptome generated by Rivera and Davies (2021) using bowtie2 (Langmead and Salzberg 2012) to report the best of all possible alignments. A custom Perl script (samcount.pl, see Data Accessibility statement) was used to enumerate the number of reads mapping to coral and symbiont contigs. Counts files for each sample were then imported into R v. 4.1.1 (R Core Team 2020) for further analyses (see Data Accessibility statement for script availability). Only gene counts for the coral host were analyzed as the algal symbiont had too few counts to ensure robust analyses.

Host gene counts across samples varied substantially (from 1,315 to 81,1642) and seven samples had fewer than 30,000 counts across all genes and were removed from downstream analyses. 23,016 host contigs and 16 samples were retained for further analysis (Table 1).

Differentially expressed genes (DEGs) were identified using DESeq2 v.1.34.0 (Love et al. 2014) in R v.4.1.1 using the model: *design = ~treatment*. Genotype was not included as a factor in the model due to the inconsistent representation of genotypes across treatments stemming from RNA extraction failure or lack of read depth (see above). Contigs were considered a DEG if the corresponding treatment contrasts had an FDR-adjusted *p*-value <0.1. Using the results() function of DESeq2, each challenge treatment was contrasted to the fed ambient treatment as this represented the control condition for both feeding and temperature challenges. Counts were normalized using the *rlog* transformation function in DESeq2 and visualized via a PCA using the prcomp() function in R. The effect of treatment was tested using a PERMANOVA with the adonis() function in the R package *vegan* using Euclidean distances between samples.

Functional differences in gene expression between treatments were further explored using gene ontology (GO) enrichment analysis using the rank-based Mann–Whitney *U*-test (MWU) approach employed by the GO-MWU package (Wright et al. 2015). This approach identified GO terms that were significantly enriched among up/downregulated genes in each pairwise contrast. The test for enrichment of GO terms was based on the ranked −*log* signed *p*-values of each gene for each of the three treatment contrasts. Similarities in GO enrichment patterns between treatments were explored by correlating the GO delta rank results from GO-MWU for pairs of treatments. A heatmap of significant DEGs was generated using the *pheatmap* package (Kolde 2012) in R.

Table 1. TagSeq generated reads and gene counts for samples.

Sample	Genet	Treatment	Raw reads	Trimmed reads	Gene counts
B1	B	fed, ambient	6,102,730	1,153,388	180,855
B2	B	fed, heated	5,072,060	962,119	148,620
B5*	B	unfed, heated	22,042	8,730	1,537
B8	B	unfed, ambient	12,065,915	1,887,341	297,235
C2	C	unfed, ambient	977,428	271,088	47,455
C4*	C	fed, heated	88,574	26,284	3,872
E3*	AE	fed, ambient	562,469	123,591	11,104
G1*	G	unfed, ambient	52,802	16,995	2,121
G3	G	unfed, heated	367,203	138,143	30,335
I5	I	unfed, ambient	3,674,235	604,045	84,049
J13	J	fed, heated	17,560,389	3,259,333	811,642
J15	J	fed, ambient	11,100,419	1,857,042	347,231
J9	J	unfed, heated	7,327,770	1,625,309	396,993
L4	L	unfed, ambient	2,411,213	617,938	110,910
M1*	M	unfed, heated	14,012	6,922	1,315
M5	M	fed, ambient	6,519,181	1,134,814	209,896
N14	N	fed, heated	8,625,195	1,966,392	445,580
N4	N	unfed, ambient	8,865,376	1,064,397	165,288
O11*	O	fed, heated	106,229	29,161	3,617
Q1	Q	fed, ambient	10,736,660	1,207,911	197,692
Q6	Q	fed, heated	2,762,352	715,139	220,261
R2*	R	fed, heated	437,647	126,978	20,984
R7	R	fed, ambient	5,046,371	908,680	152,505

Raw reads: total number of reads generated for the sample during sequencing. Trimmed reads: numbers of reads remaining after trimming and quality filtering (see methods). Gene Counts: number of reads mapping to *O. arbuscula* transcriptome. Samples with * were dropped from further analyses due to low gene counts.

Results

Feeding had a limited effect in mitigating declines in symbiont physiology metrics

Overall heat challenge caused a significant reduction in photosynthetic efficiency of photosystem II (F_v/F_m) of *O. arbuscula* algal symbionts by 31 °C regardless of feeding regime (experimental day 22, $p < 0.01$). This effect was even stronger at the end of the experiment after reaching peak (33 °C) temperatures (experimental day 28, $p < 0.001$). Feeding did not mitigate this decline in F_v/F_m as both heated treatments were indistinguishable from one another throughout the experiment (Fig. 2A).

Symbiont densities were less impacted by treatment than other symbiont physiological conditions. Symbiont cell densities were greatest under unfed, ambient temperature conditions with the unfed, heated treatments exhibiting significantly lower density relative to the unfed, ambient treatment ($p = 0.037$; Fig. 2B). Feeding may have helped maintain marginally higher densities under heated temperatures, as the fed, heated treatment did not show significantly lower densities than either ambient temperature treatment.

Chlorophyll-a concentrations were significantly higher in both ambient conditions relative to both heated treatments ($p < 0.05$ for all comparisons). No differences were observed between unfed, ambient and fed, ambient conditions ($p > 0.6$; Fig. 2C). For chlorophyll-c_2, feeding may have marginally mitigated loss under heated conditions, as there were no significant differences between either ambient treatments and the fed, heated treatment (Fig. 2D). However, this may have been due only to the two samples with much higher chlorophyll-c_2 levels as the median of both heated treatments is very similar and lower than both ambient temperature treatments (Fig. 2D).

Symbiont protein concentrations were comparable among all treatments and showed no response to any treatment (Fig. 2F). In contrast, symbiont carbohydrates were significantly higher under fed, ambient conditions relative to all other treatments ($p < 0.05$ for all contrasts), though there was a trend toward further declines in carbohydrate reserves with increasing treatment challenge (i.e. temperature and lack of feeding; Fig. 2H).

Coral host energy reserves showed increasing response to lack of feeding and higher temperatures

Host protein levels were significantly lower in every treatment relative to the fed, ambient control ($p < 0.05$ for all contrasts; Fig. 2E). Feeding may have provided some mild relief to protein levels under heated conditions as fed, heated samples did not differ from unfed, ambient (Fig 2E); however, they were also not statistically different from unfed, heated corals. Any potentially mitigating effect of feeding is, therefore, very small. Host carbohydrate concentrations, on the hand, did not differ across any of the experimental treatments (Fig. 2G).

Elevated temperatures resulted in more pronounced physiological changes for both coral and symbiont

When investigating all phenotypes using a PCA, we observe that coral holobiont phenotypes were significantly different across conditions, with the most pronounced divergence between ambient and heated conditions ($P_{treatment} < 0.001$; Fig. 3). Overall, we observe that the influence of heat was much greater on coral holobiont phenotypes than food availability.

Elevated temperatures elicit stronger gene expression responses than feeding limitation

A PCA of all *O. arbuscula rlog*-normalized genes showed that temperature had a significant effect on gene expression ($p < 0.001$), while heterotrophy did not ($p = 0.2$; Fig. 4A). Pairwise comparisons between each experimental treatment relative to fed, ambient conditions showed no DEGs in unfed, ambient samples, while the largest number of DEGs was observed in fed, heated (Fig. 4B). However, it should be noted that only two samples were retained in the unfed, heated treatment, as such that comparison is underpowered and the number of DEGs may be underestimated.

Heat-challenged corals had convergent gene expression responses regardless of feeding treatment

DEGs in the unfed, heated treatment largely overlapped with genes that were also differentially expressed in the fed, heated treatment, with 74 (25 upregulated, 49 downregulated) of the 94 DEGs in unfed, heated also being DEGs in the fed, heated treatment (Fig. 4B). Overlapping genes showed consistent levels of expression in both unfed and fed, heated treatments relative to the fed, ambient control (Fig. 5A). Of note, this gene set included several upregulated calumenin and heat-shock proteins and several downregulated amino acid and lipid transporter proteins (Fig. 5A).

Significantly enriched GO functional terms were also consistent between unfed and fed, heated samples (Fig. 5B). In both heated treatments, regardless of feeding treatment, biological processes associated with ion and amino acid transport were underrepresented as were cell signaling pathways, action potentials, and regulation of secretion (Fig. 5B). Conversely, biological processes including protein folding, RNA processing, DNA regulation and repair, and catabolism were overrepresented (Fig. 5B).

Unfed, heated corals upregulated cell cycle control

Despite largely similar gene expression responses between unfed and fed, heat-challenged samples, unfed, heated samples had 55 unique significantly enriched biological process GO terms that were not enriched in fed, heated samples. Over a third of these terms were associated with cell cycle regulation and telomere maintenance (Fig. 6). Most other GO terms, while unique to unfed, heated samples, were closely related to other GO terms that were shared between unfed and fed, heated samples such as homeostasis, secretion, and response to stimulus or stress (Figs. 5 and 6).

Unfed, ambient samples upregulated cilia-related GO biological processes

Although unfed, ambient samples did not show any significantly DEGs relative to fed, ambient control, GO enrichment analysis identified a small number of significantly enriched biological process terms, most of which were associated with cilia development and cell motility (Fig. S2).

Discussion

Short-term starvation has limited impact in the absence of additional challenges

In agreement with prior studies (Aichelman et al. 2016; Levy et al. 2016; Fong et al. 2021), we found that feeding intensity (i.e. fed, ambient vs. unfed, ambient) had a limited impact on most coral and algal physiology metrics in the absence of heat challenge (Fig. 2). Host protein reserves in unfed, ambient corals did show a decline relative to fed, ambient controls (Fig. 2E). Given that all corals were fed regularly prior to the start of the experiment, it may have been that the starvation period used here was insufficient to elicit stronger declines in coral host energy reserves. We did observe a significant decline in symbiont carbohydrate (but not symbiont protein) reserves under unfed, ambient conditions (Fig. 2H), suggesting that the host may have been using more symbiont-derived carbohydrates to compensate for declines in food availability, while catabolizing some of its own protein reserves (Fig. 2E, H). A prior heat stress and feeding study using *Stylophora pistilla* found more symbiont-derived carbohydrates were transferred to the host in unfed conditions (Tremblay et al. 2016), which is consistent with our physiological observations.

Although we found no DEGs in unfed, ambient relative to fed, ambient conditions, GO analyses did reveal several enriched biological processes (Fig. S2). Among these, several cilia-associated terms were overrepresented, suggesting unfed, ambient corals may have been increasing feeding behavior to compensate for lower food availability. In addition, immune response and complement activation GO terms were also overrepresented in unfed, ambient corals (Fig. S2). Prior work examining gene expression differences between symbiotic and aposymbiotic *O. arbuscula* found upregulation of immune response in aposymbiotic branches (Rivera and Davies 2021); a pattern also observed in other facultatively symbiotic species (Burns et al. 2017; Cui et al. 2019). Although symbiont densities were maintained in unfed, ambient samples, overrepresentation of immune response terms could signal the onset of the bleaching response, which can be characterized by an overproliferation of symbionts during early stages (Wooldridge 2013). It is possible that if starvation conditions were sustained longer, we may have observed reductions in symbiont densities in unfed corals, which would be consistent with coral bleaching.

Heterotrophy did little to mitigate the impacts of heat challenge

Although prior studies in *O. arbuscula* showed that heterotrophy can mitigate symbiont loss and calcification declines (Aichelman et al. 2016), we found minimal evidence for such an effect here. Symbiont densities were slightly, though not significantly, lower in unfed, heated corals relative to both fed, heated and fed, ambient corals (Fig. 2B). Conversely, unfed, ambient corals showed the highest densities, suggesting interactions between feeding levels and symbiont densities were complicated (Fig. 2B). A prior study on the tropical coral *Pocillopora acuta* also found trends of higher symbiont densities in unfed, unstressed conditions (Fong et al. 2021). Interestingly, symbiont densities did not decline substantially
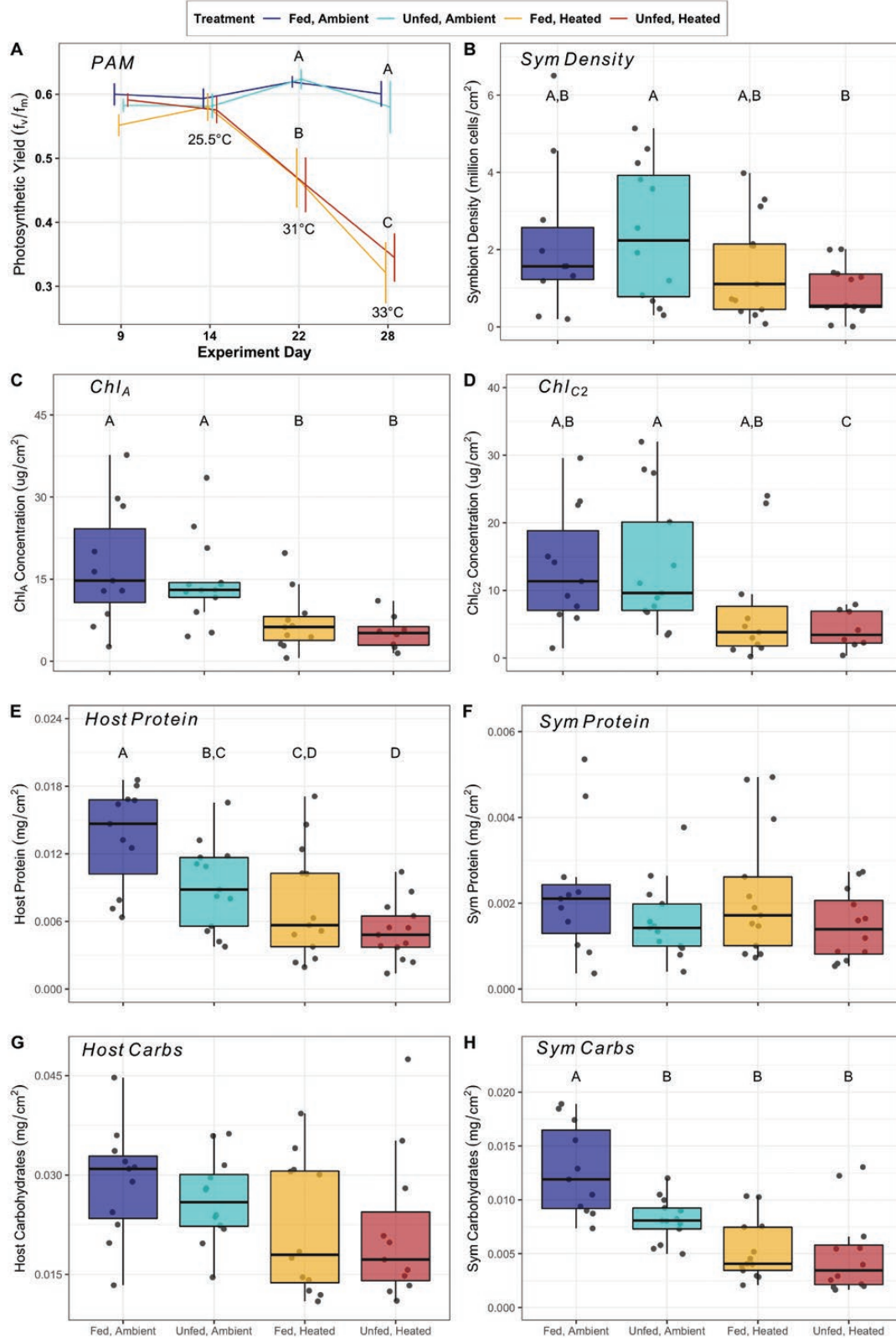
Fig. 2. *Oculina arbuscula* phenotypic data across treatments: (A) Photosynthetic efficiency of photosystem II of algal symbionts (F_v/F_m) through time shown as treatment mean +/− standard error. Average temperature during the day of F_v/F_m measurement is shown for both heated treatments after the start of the heat ramp. Refer to Fig. 1B for the full temperature time series. (B–H) Phenotypic differences observed across treatments at the end of the experiment (day 28). Box plots denote treatment medians (black bar) and interquartile range (rectangle). All sample data are shown as jittered points behind each box plot. (B) symbiont density (million cells/cm^2), (C) chlorophyll-a concentration (ug/cm^2), (D) chlorophyll-c$_2$ concentration (ug/cm^2), (D) host protein (ug/cm^2), (E) host carbohydrate (ug/cm^2), (F) symbiont protein (ug/cm^2), and (G) symbiont carbohydrate (ug/cm^2). All measurements are normalized to live coral surface area. Data were analyzed as generalized linear models with genotype as random effects to account for genotype driven responses across treatments. Letters indicate significant differences ($p < 0.05$) between treatments based on post hoc Tukey tests.
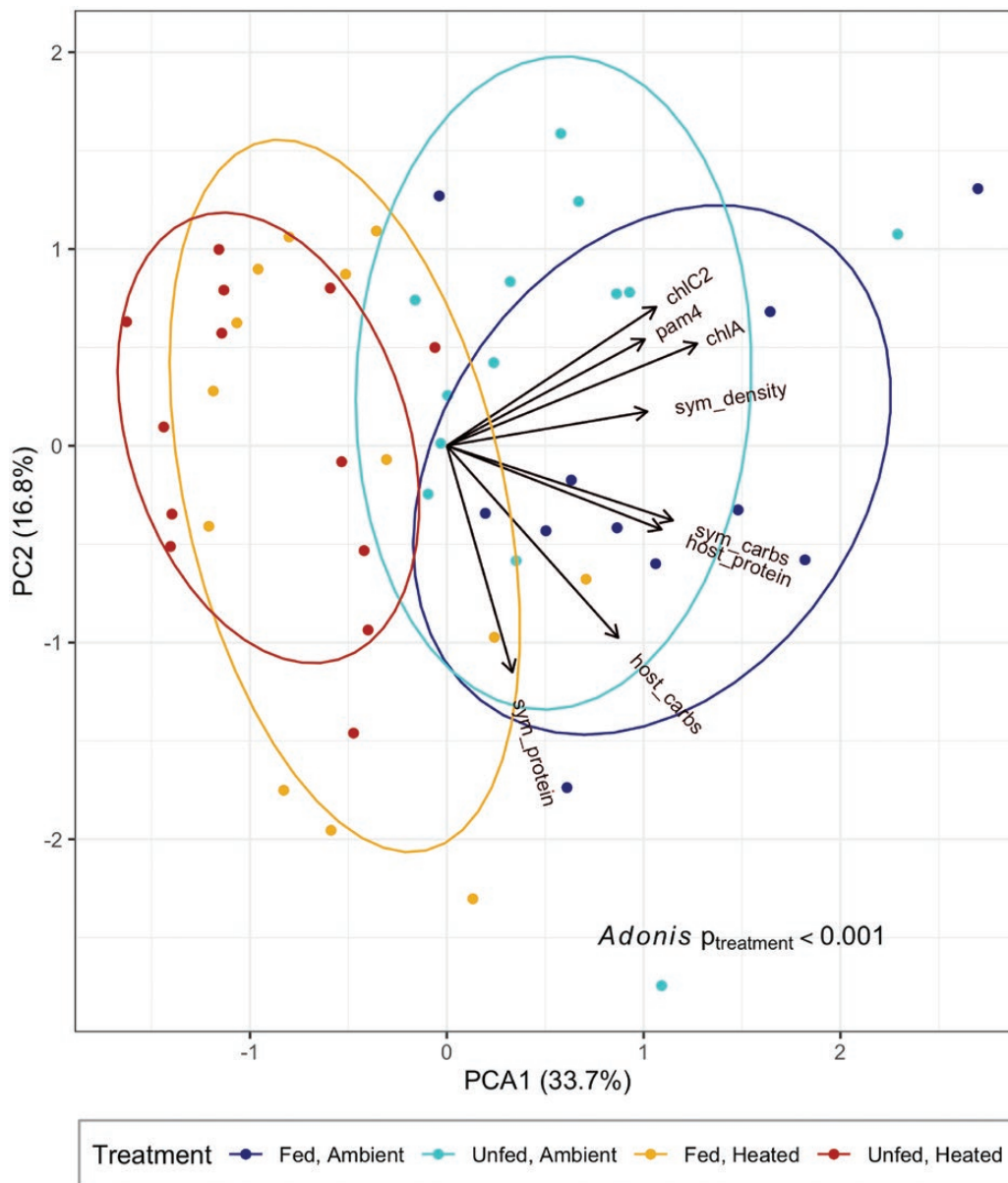
Fig. 3. Influence of experimental treatments on *Oculina arbuscula* holobiont phenotypes. Principal components analyses of holobiont phenotypic data, including total host carbohydrate (host, carbs; mg/cm^2), total symbiont carbohydrate (sym, carbs; mg/cm^2), total host protein (host, protein; mg/cm^2), total symbiont protein (sym, protein; mg/cm^2), symbiont density (sym, density; cells/cm^2), chlorophyll-a (chlA; µg/cm^2), chlorophyll-c2 (chlC2; µg/cm^2), and "pam" for the photosynthetic efficiency of photosystem II of algal symbionts (F_v/F_m) at the end of the experiment (day 28). Points represent an individual coral fragment's physiology. The *x*- and *y*-axes indicate variance explained (%) by the first and second principal components, respectively.

in heat-challenged corals, despite more sharp declines in symbiont photosynthetic efficiency (Fig. 2A, B). While these findings appear somewhat surprising, such patterns have been previously described in several coral species during short-term heat challenges (Warner et al. 1996), underscoring that the timing of these measurements is important.

Differences in experimental and acclimation timelines between *O. arbuscula* experiments may have limited the mitigating benefits of increased heterotrophy against bleaching. Our experimental colonies were collected from the same site and population as those used in (Aichelman et al. 2016), and as such could be expected to have similar feeding patterns and responses. However, experimental fragments in Aichelman et al. (2016) were fed live *Artemia nauplii*, whereas we fed the fragments Reef-Roids™ in order to feed

each fragment individually and have more precise control over portion allocation. Regardless the amount of food or the nutrition, this food source provided may have been insufficient to elicit the same mitigating benefits as live *A. nauplii*. In addition, our fragments were lab acclimated for over a year, during which they were fed regularly, while those used in Aichelman et al. (2016) were used within 1 mo of collection. Therefore, fragments assigned to our unfed treatment likely had higher energy reserves going into the experiment due to longer lab acclimation and feeding regimes than the winter-collected wild corals used in Aichelman et al. (2016). Our longer timing likely minimized the immediate influence of food availability on the coral bleaching response. In addition, *O. arbuscula* has been shown to have different prey capture rates and efficiency depending on food size and flow,
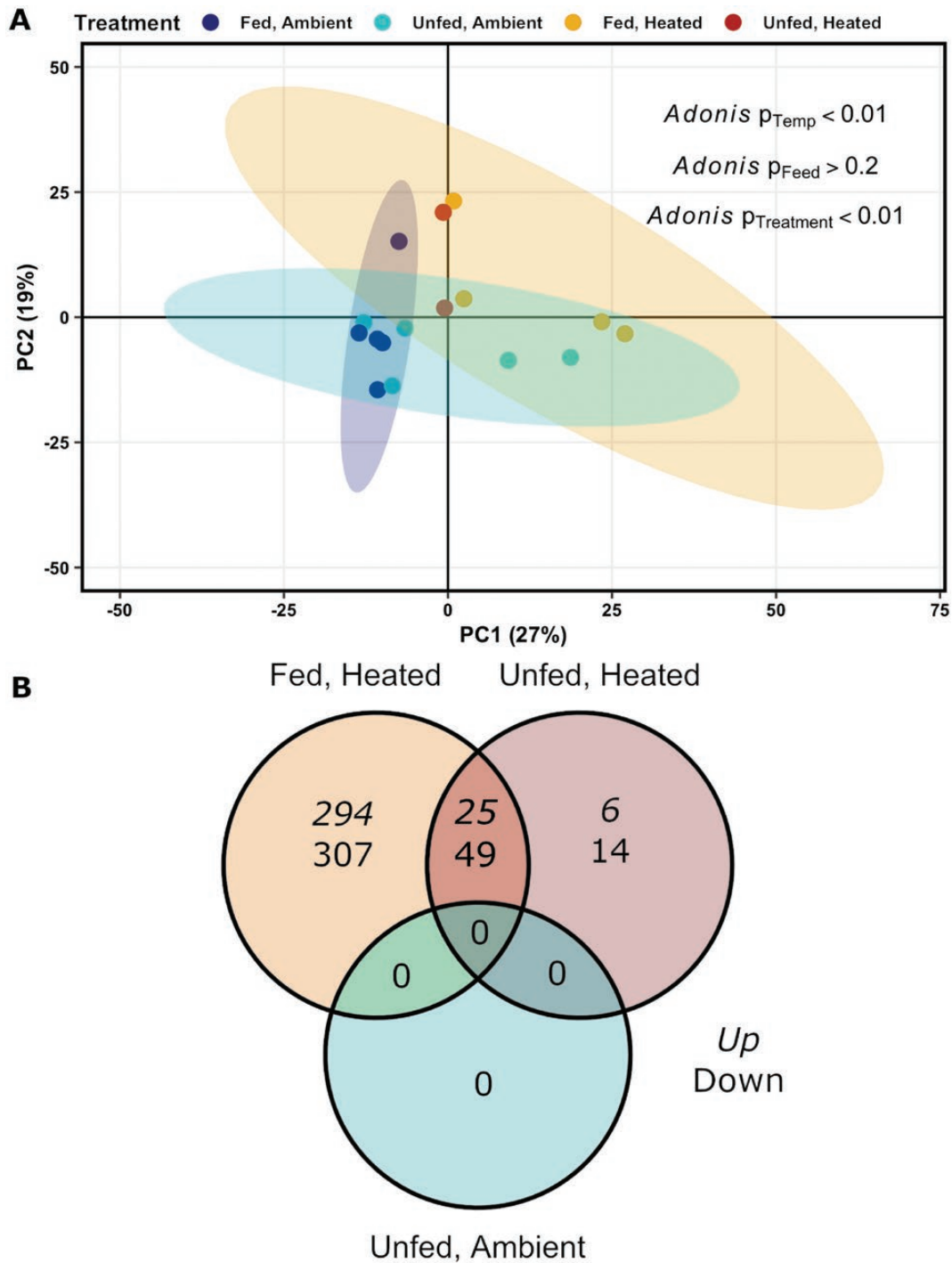
Fig. 4. *Oculina arbuscula* host gene expression differences across treatments: (A) Principal component analyses of *rlog*-transformed counts for all genes. PERMANOVA results for the effect of experimental treatments are shown. (B) Venn diagram of up- (italicized) and downregulated genes across all pairwise treatments relative to control (fed, ambient) conditions (P_{FDR} = 0.10). A total of 601 genes were uniquely differentially expressed in the fed, heated treatment (294 up, 307 down), while 20 were uniquely differentially expressed in the unfed, heated treatment (6 up, 14 down). Seventy-four genes were common to both heated treatments (25 upregulated, 49 downregulated). The unfed, ambient treatment did not have any differentially expressed genes relative to the fed, ambient.

with lower rates and efficiency at smaller prey size ([Piniak 2002](#)). A prior study on another facultative, temperate coral, *Astrangia poculata*, also found that feeding behavior and polyp extension are suppressed under temperature challenges ([Wuitchik et al. 2021](#)). The small Reef-Roids™ powder particles may have been less effectively captured by fragments,

and a decline in feeding behavior under heat challenge may have further limited food intake and therefore limited the capacity for heterotrophy to mitigate the impacts of heat stress. Future experiments on lab-acclimated corals should consider prolonging the starvation period and relying on larger live food options to ensure appropriate food provisioning.
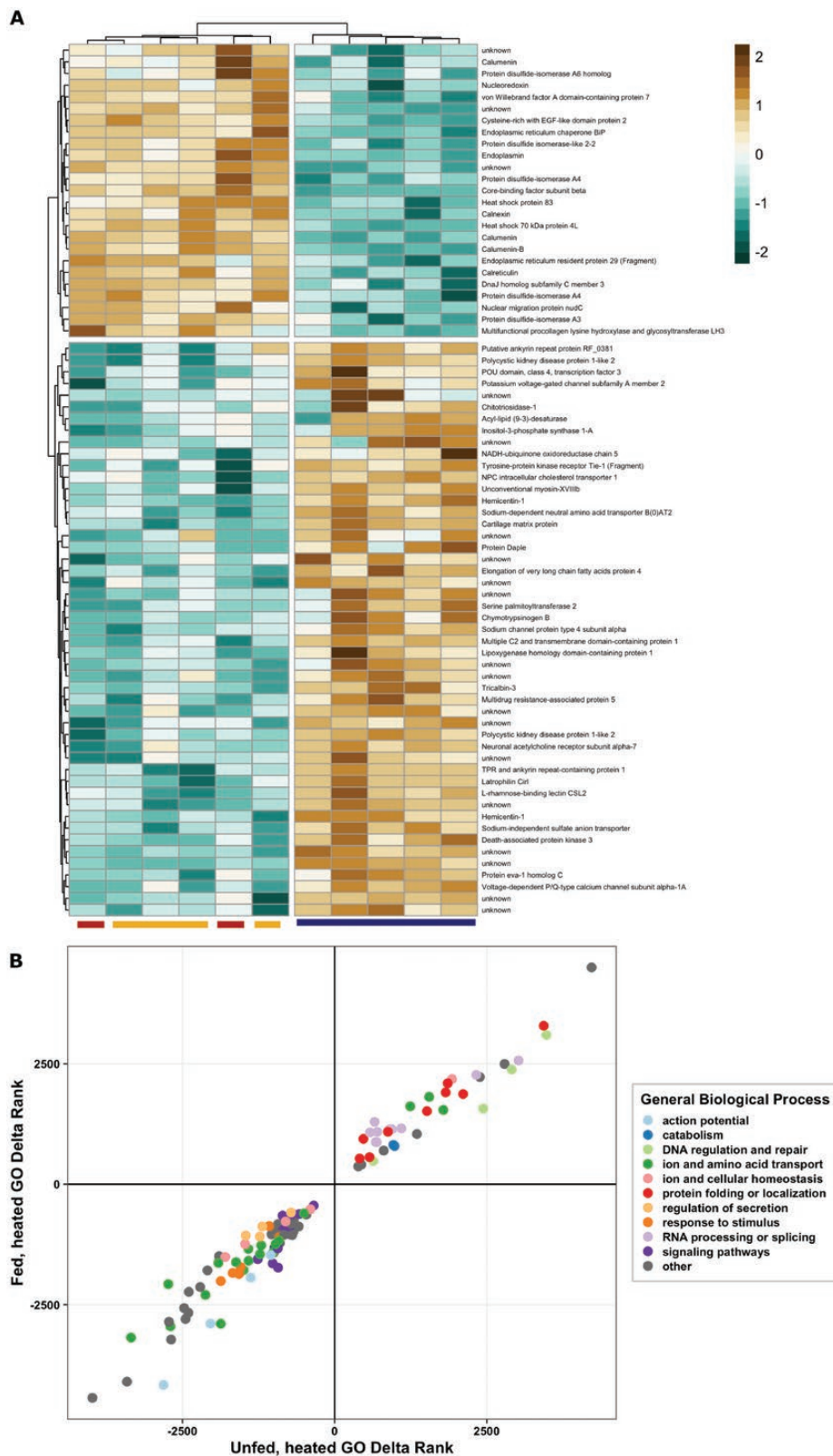
Fig. 5. Consistent gene expression responses in unfed and fed, heated samples relative to fed, ambient controls. (A) Heatmap of shared differentially expressed genes (*N* = 74) in unfed and fed, heated treatments relative to fed, ambient control. Color scale represents the *rlog*-normalized expression scaled within rows as a deviation from the row mean. Gene name is listed for each row. Unannotated genes are designated as unknown. Rows and columns are clustered hierarchically using Pearson correlation of their expression levels across genes and samples. Heated samples are all clustered on the left, separately from fed, ambient controls. Color blocks along the bottom correspond to treatment colors used throughout. (B) Comparison of biological process gene ontology (GO) delta ranks of significantly enriched GO categories shared by samples in unfed, heated and fed, heated relative to fed, ambient control. Positive ranks are categories that are overrepresented with upregulated genes (higher expression in heated samples relative to fed, ambient control), while negative ranks are underrepresented GO categories. Colors of points correspond to general Biological Process categories for ease of visualization. See Table S1 the full names of terms represented in the figure.

Fig. 6. Biological process gene ontology (GO) delta ranks of significantly enriched GO categories that are uniquely responding to the dual stressors of being unfed and heated. Positive (pointing outwards) bars are enriched categories associated with upregulated genes (higher expression in unfed, heated relative to fed, ambient control samples), while negative (pointing inwards) bars are underrepresented GO categories that signify pathways that are downregulated under multiple stressors (unfed, heated). Colors of points correspond to general Biological Process categories for ease of visualization. Some words were shortened to ease visualization: org: organization; reg: regulation; +: positive; −: negative; maint.: maintenance; proc: process. See Table S2 the full names of terms represented in the figure.

Gene expression response recapitulates transcriptomic environmental stress response signatures independent of feeding regime

In both heat-challenged treatments, the major gene expression patterns aligned with previously reported heat-stress responses, such as upregulation of heat-shock proteins and enrichment of ion transport and stress response GO terms (reviewed in Cziesielski et al. 2019). The lack of a strong gene expression signature for starvation could be the result of insufficient starvation, which is discussed above. Alternatively, starvation could elicit more subtle gene expression shifts unless combined with other challenges. For instance, Levy et al.

(2016) found a stronger transcriptional response in unfed, high-light stress samples than those in a fed, high-light stress treatment, relative to fed, control temperatures in *Stylophora pistillata*; but only two DEGs between feeding treatments under control light conditions. In addition, only two samples from the unfed, heated treatment resulted in successful library preparation for gene expression analyses. If mild starvation stress elicits more subtle gene expression changes than heat stress in *O. arbuscula*—as suggested by the lack of differential expression between unfed and fed samples, in ambient temperatures—our analysis would be unlikely to detect these subtle changes in unfed, heated samples due to limited power from the small sample size.

Heat challenge and starvation, respectively, may also prompt the stronger type A and milder type B gene expression responses described in Dixon et al. (2020). Heat challenge should present a more immediate and acute stressor than starvation in a mixotrophic organism such as corals, which relies heavily on autotrophically derived carbohydrates from its symbiont (Muscatine et al. 1981). Though one may expect a stronger reliance on food availability in a facultatively symbiotic coral, such as *O. arbuscula*, the starvation treatment in this experiment may not have been sufficient to induce a stress response. In addition, since *O. arbuscula* can survive in a fully aposymbiotic state, even a lower density of symbionts may be sufficient to meet most of its energetic needs thereby limiting the impact of starvation when it's in a symbiotic state. In fact, a field study of *O. arbuscula* found that symbiotic colonies derive most of their nutrition from endosymbionts, regardless of season, suggesting that even during darker months when photosynthesis is limited and symbiont density is lower, symbionts produced sufficient sugars to maintain coral host health (Leal et al. 2014). Furthermore, type B gene expression changes are often more subtle and in the opposite direction of type A responses (Dixon et al. 2020), making type B responses more difficult to detect if combined with a stressor that induces a type A gene expression response. The only enriched biological process GO categories that were unique to unfed, heated samples were related to cell division and DNA replication ("cell cycle" in Fig. 6). Both of these are categories that are often enriched amongst upregulated genes in type B response (Dixon et al. 2020), suggesting starvation could be eliciting a type B response in our study. In addition, ciliary flows can enhance aeration and mass transport including nutrient exchange by generating the mixing of the coral boundary layer and as such can be beneficial for both enhancing photosynthesis and enabling prey capture (Shapiro et al. 2014; Pacherres Reaño 2021). Enrichment of cilia-related biological process GO terms in unfed, ambient samples suggest that corals may have only been beginning to feel the effects of starvation and, in response, initiated cilia development to facilitate additional food capture.

While it is possible that both temperature challenge and starvation can elicit type A responses—which yield similar gene expression changes regardless of the stressor ((Dixon et al. 2020)—starvation in our experiment had little effect on any physiological metrics under ambient conditions, indicating that our starvation treatment was mild (Figs. 2 and 3). In an experiment using *Stylophora pistillata* examining light stress and starvation, Levy et al. (2016) also found that starvation under nonstress light conditions yielded no differences in coral host and symbiont physiology and no significant gene expression differences (except for two genes with less than a

2-fold change in expression), providing some support to the notion that starvation may instead induce a type B response. Future heterotrophy-based experiments seeking to understand the molecular changes associated with starvation itself should take additional care to ensure that starvation is sufficient by testing different feeding levels (e.g. Aichelman et al. 2016).

Conclusions

O. arbuscula is a well-suited model for investigating the role of heterotrophy in modulating bleaching responses and temperature tolerance (Rivera and Davies 2021). If starvation indeed elicits type B stress responses in corals, decoupling the effects of starvation, or conversely increased heterotrophy, on symbiosis dynamics and coral thermal tolerance can be challenging. *Oculina arbuscula* is a facultatively symbiotic coral and gene expression signatures of its symbiotic and aposymbiotic states have been previously described (Rivera and Davies 2021). Prior studies have suggested that as ocean temperatures continue to rise, corals that can more easily shift to heterotrophy may be better equipped to survive bleaching events (Grottoli et al. 2006; Hughes and Grottoli 2013; Conti-Jerpe et al. 2020). Our study provides a framework for further exploration of such effects using a facultatively symbiotic coral and also underscores that the effect of increased heterotrophy in mitigating bleaching impacts may be more nuanced than previously thought. Factors such as the type of food available, the level of energetic reserves available to the coral prior to the onset of bleaching stress, and the duration of the stressor could all limit the beneficial effects of higher food availability. Future experiments that examine the role of heterotrophy across symbiotic and aposymbiotic states in combination with other stressors of interest such as temperature, acidification, or irradiance levels will allow for a more nuanced exploration of the molecular mechanisms that underpin the impacts of heterotrophy on stress responses in reef-building corals. Studies that incorporate physiological understanding and the evolutionary potential of species in responding to a variety of climate stressors can provide more accurate estimates of extinction risk and better inform conservation decisions (Forester et al. 2022). As coral reefs face mounting extinction pressure from increasing ocean temperatures, policy-makers and conservation leaders will face tough choices on how to allocate resources for time-intensive and expensive restoration efforts. Knowing whether corals that can resort to increase heterotrophy may face better odds of survival will be key information for proper management.

Supplementary Material

Supplementary material can be found at http://www.jhered.oxfordjournals.org/.

Funding

Acknowledgments

Author Contributions

Conceptualization and Methodology: HER and SWD. Formal Analysis: HER and SWD. Investigation: HER, CAT, HD, JS. Data Curation: HER. Visualization and Writing—Original Draft Preparation: HER and SWD. Writing—Review & Editing: HER, CAT, and SWD. Funding Acquisition: HER and SWD. Project Administration and Resources: SWD.

Conflict of Interest

The authors declare no conflicts of interest with the presented work.

Data Availability

Raw reads for all 23 samples are available on the NCBI Short Read Archive (SRA) under BioProject number PRJNA841352. Scripts and input data for all other analyses, for example, physiology, read mapping, differential expression, etc. are hosted at https://github.com/hrivera28/oculina_heterotrophy.

References

Aichelman HE, Townsend JE, Courtney TA, Baumann JH, Davies SW, Castillo KD. Heterotrophy mitigates the response of the temperate coral *Oculina arbuscula* to temperature stress. *Ecol Evol*. 2016:6(18):6758–6769.

Anthony KRN, Hoogenboom MO, Maynard JA, Grottoli AG, Middlebrook R. Energetics approach to predicting mortality risk from environmental stress: a case study of coral bleaching. *Funct Ecol*. 2009:23(3):539–550.

Avila-Magaña V, Kamel B, DeSalvo M, Gómez-Campo K, Enríquez S, Kitano H, Rohlfs RV, Iglesias-Prieto R, Medina M. Elucidating gene expression adaptation of phylogenetically divergent coral holobionts under heat stress. *Nat Commun*. 2021:12:5731.

Barott KL, Venn AA, Perez SO, Tambutté S, Tresguerres M. Coral host cells acidify symbiotic algal microenvironment to promote photosynthesis. *Proc Natl Acad Sci USA*. 2015:112(2):607–612.

Barshis DJ, Ladner JT, Oliver TA, Seneca FO, Traylor-Knowles N, Palumbi SR. Genomic basis for coral resilience to climate change. *Proc Natl Acad Sci USA*. 2013:110(4):1387–1392.

Bay LK, Guérécheau A, Andreakis N, Ulstrup KE, Matz MV. Gene expression signatures of energetic acclimatisation in the reef building coral *Acropora millepora*. *PLoS One*. 2013:8(5):e61736.

Burmester EM, Breef-Pilz A, Lawrence NF, Kaufman L, Finnerty JR, Rotjan RD. The impact of autotrophic versus heterotrophic nutritional pathways on colony health and wound recovery in corals. *Ecol Evol*. 2018:8(22):10805–10816.

Burns JA, Zhang H, Hill E, Kim E, Kerney R. Transcriptome analysis illuminates the nature of the intracellular interaction in a vertebrate-algal symbiosis. *Elife*. 2017:6:e22054.

Conlan JA, Humphrey CA, Severati A, Francis DS. Influence of different feeding regimes on the survival, growth, and biochemical composition of Acropora coral recruits. *PLoS One*. 2017:12(11):e0188568.

Conti-Jerpe IE, Thompson PD, Wong CWM, Oliveira NL, Duprey NN, Moynihan MA, Baker DM. Trophic strategy and bleaching resistance in reef-building corals. *Sci Adv*. 2020:6(15):eaaz5443.

Cui G, Liew YJ, Li Y, Kharbatia N, Zahran NI, Emwas A-H, Eguiluz VM, Aranda M. Host-dependent nitrogen recycling as a mechanism of symbiont control in Aiptasia. *PLoS Genet*. 2019:15(6):e1008189.

Cziesielski MJ, Schmidt-Roach S, Aranda M. The past, present, and future of coral heat stress studies. *Ecol Evol*. 2019:9:10055–10066.

Davies SW, Marchetti A, Ries JB, Castillo KD. Thermal and pCO_2 stress elicit divergent transcriptomic responses in a resilient coral. *Front Mar Sci*. 2016:3.

Dixon G, Abbott E, Matz M. Meta-analysis of the coral environmental stress response: Acropora corals show opposing responses depending on stress intensity. *Mol Ecol*. 2020:29(15):2855–2870.

Dixon GB, Davies SW, Aglyamova GA, Meyer E, Bay LK, Matz MV. Genomic determinants of coral heat tolerance across latitudes. *Science*. 2015:348(6242):1460–1462.

Fong J, Poquita-Du RC, Todd PA. Plastic responses in the coral *Pocillopora acuta* to extreme low-light conditions with and without food provision. *Mar Biol*. 2021:168(113):113.

Forester BR, Beever EA, Darst C, Szymanski J, Funk WC. Linking evolutionary potential to extinction risk: application and future directions. *Front Ecol Environ*. 2022. doi:10.1002/fee.2552

Glynn PW. Coral reef bleaching: facts, hypotheses and implications. *Glob Chang Biol*. 1996:2(6):495–509.

Grottoli AG, Rodrigues LJ, Palardy JE. Heterotrophic plasticity and resilience in bleached corals. *Nature*. 2006:440:1186–1189.

Hawkins TD, Krueger T, Wilkinson SP, Fisher PL, Davy SK. Antioxidant responses to heat and light stress differ with habitat in a common reef coral. *Coral Reefs*. 2015:34:1229–1241.

Hothorn T, Bretz F, Westfall P. Simultaneous inference in general parametric models. *Biom J*. 2008;50(3):346–363.

Houlbrèque F, Ferrier-Pagès C. Heterotrophy in tropical scleractinian corals. *Biol Rev Camb Philos Soc*. 2009:84(1):1–17.

Hughes TP, Barnes ML, Bellwood DR, Cinner JE, Cumming GS, Jackson JBC, Kleypas J, van de Leemput IA, Lough JM Morrison TH et al. Coral reefs in the Anthropocene. *Nature* 2017;546:82–90. doi:10.1038/nature22901.

Hughes AD, Grottoli AG. Heterotrophic compensation: a possible mechanism for resilience of coral reefs to global warming or a sign of prolonged stress? *PLoS One*. 2013:8(11):e81172.

Hughes TP, Kerry JT, Baird AH, Connolly SR, Dietzel A, Eakin CM, Heron SF, Hoey AS, Hoogenboom MO, Liu G, et al. Global warming transforms coral reef assemblages. *Nature*. 2018:556:492–496.

Jeffrey S, Haxo FT. Photosynthetic pigments of symbiotic dinoflagellates (zooxanthellae) from corals and clams. *Biol. Bull*. 1968:135:149–165.

Kolde R. *Pheatmap: pretty heatmaps*. 2012. R Package Version 1.0.10. https://CRAN.R-project.org/package=pheatmap.

Langmead B, Salzberg SL. Fast gapped-read alignment with Bowtie 2. *Nat Methods*. 2012:9:357–359.

Leal MC, Ferrier-Pagès C, Calado R, Brandes JA, Frischer ME, Nejstgaard JC. Trophic ecology of the facultative symbiotic coral *Oculina arbuscula*. *Mar Ecol Prog Ser*. 2014:504:171–179.

Levy O, Karako-Lampert S, Waldman Ben-Asher H, Zoccola D, Pagès G, Ferrier-Pagès C. Molecular assessment of the effect of light and heterotrophy in the scleractinian coral *Stylophora pistillata*. *Proc Biol Sci*. 2016:283(1829).

Love MI, Huber W, Anders S. Moderated estimation of fold change and dispersion for RNA-seq data with DESeq2. *Genome Biol*. 2014:15(2014):550.

Masuko T, Minami A, Iwasaki N, Majima T, Nishimura S-I, Lee YC. Carbohydrate analysis by a phenol–sulfuric acid method in microplate format. *Anal. Biochem*. 2005:339:69–72. doi:10.1016/j.ab.2004.12.001

Meyer E, Aglyamova GV, Matz MV. Profiling gene expression responses of coral larvae (*Acropora millepora*) to elevated temperature and settlement inducers using a novel RNA-Seq procedure. *Mol Ecol*. 2011:20(17):3599–3616.

Miller MW. Growth of a temperate coral: effects of temperature, light, depth, and heterotrophy. *Mar Ecol Prog Ser*. 1995:122:217–225.

Morris LA, Voolstra CR, Quigley KM, Bourne DG, Bay LK. Nutrient availability and metabolism affect the stability of coral-symbiodiniaceae symbioses. *Trends Microbiol*. 2019:27(8):678–689.

Muscatine, L. The role of symbiotic algae in carbon and energy flux in reef corals. In: Dubinsky Z, editor. *Coral Reefs*. Amsterdam: Elsevier; 1990, pp. 75–87.

Muscatine L, Cernichiari E. Assimilation of photosynthetic products of zooxanthellae by a reef coral. *Biol Bull*. 1969:137:506–523.

Muscatine L, McCloskey L R, Marian R E. Estimating the daily contribution of carbon from zooxanthellae to coral animal respiration. *Limnol Oceanogr*. 1981:26(4):601–611.

Muscatine L, Porter JW. Reef corals: mutualistic symbioses adapted to nutrient-poor environments. *Bioscience*. 1977:27(7):454–460.

Normile D. El Niño's warmth devastating reefs worldwide. *Science*. 2016:352(6281):15–16.

Pacherres Reaño CO. *The role of ciliary vortices on the coral's oxygen exchange and food capture* [*PhD thesis*]. University of Bremen and Alfred Wegener Institute Helmholtz Center for Polar and Marine Research; 2021.

Pernice M, Hughes DJ. Forecasting global coral bleaching. *Nat Clim Change*. 2019:9:803–804.

Piniak G. Effects of symbiotic status, flow speed, and prey type on prey capture by the facultatively symbiotic temperate coral *Oculina arbuscula*. *Mar Biol*. 2002:141:449–455.

R Core Team. R: a language and environment for statistical computing; 2020.

Reynaud-Vaganay S, Ferrier-Pagès C, Sambrotto R, Juillet-Leclerc A, Jaubert J. Effect of feeding on the carbon and oxygen isotopic composition in the tissues and skeleton of the Zooxanthellate coral *Stylophora pistillata*. *Mar Eco Prog Ser*. 2002;238:1–89.

Rivera HE, Davies SW. Symbiosis maintenance in the facultative coral, *Oculina arbuscula*, relies on nitrogen cycling, cell cycle modulation, and immunity. *Sci Rep*. 2021;11:21226.

Rodolfo-Metalpa R, Peirano A, Houlbrèque F, Abbate M, Ferrier-Pagès C. Effects of temperature, light and heterotrophy on the growth rate and budding of the temperate coral *Cladocora caespitosa*. *Coral Reefs*. 2008:27:17–25.

Shapiro OH, Fernandez VI, Garren M, Guasto JS, Debaillon-Vesque FP, Kramarsky-Winter E, Vardi A, Stocker R. Vortical ciliary flows actively enhance mass transport in reef corals. *Proc Natl Acad Sci USA*. 2014:111(37):13391–13396.

Toh TC, Ng CSL, Peh JWK, Toh KB, Chou LM. Augmenting the post-transplantation growth and survivorship of juvenile scleractinian corals via nutritional enhancement. *PLoS One*. 2014:9(6):e98529.

Tremblay P, Gori A, Maguer JF, Hoogenboom M, Ferrier-Pagès C. Heterotrophy promotes the re-establishment of photosynthate translocation in a symbiotic coral after heat stress. *Sci Rep*. 2016:6:38112.

Vidal-Dupiol J, Dheilly NM, Rondon R, Grunau C, Cosseau C, Smith KM, Freitag M, Adjeroud M, Mitta G. Thermal stress triggers broad Pocillopora damicornis transcriptomic remodeling, while *Vibrio coralliilyticus* infection induces a more targeted immuno-suppression response. *PLoS One*. 2014:9(9):e107672.

Warner ME, Fitt WK, Schmidt GW. The effects of elevated temperature on the photosynthetic efficiency of zooxanthellae in hospite from four different species of reef coral: a novel approach. *Plant Cell Environ*. 1996:19(3):291–299.

Wooldridge SA. Breakdown of the coral-algae symbiosis: towards formalising a linkage between warm-water bleaching thresholds and the growth rate of the intracellular zooxanthellae. *Biogeosciences*. 2013:10(3):1647–1658.

Wright RM, Aglyamova GV, Meyer E, Matz MV. Gene expression associated with white syndromes in a reef building coral, *Acropora hyacinthus*. *BMC Genomics*. 2015:16:371.

Wuitchik DM, Almanzar A, Benson BE, Brennan S, Chavez JD, Liesegang MB, Reavis JL, Reyes CL, Schniedewind MK, Trumble IF, et al. Characterizing environmental stress responses of aposymbiotic *Astrangia poculata* to divergent thermal challenges. *Mol Ecol*. 2021:30(20):5064–5079.